The adsorption/desorption of ethanol on $Cs_xH_{3-x}PW_{12}O_{40}$ by TG/DTG-DTA analysis

O. VERDES*, L. AVRAM, A. POPA, V. SASCA
Institute of Chemistry Timisoara-Romanian Academy, Bd. M. Viteazu 24, 300223 Timisoara, Romania

The adsorption/desorption of ethanol on $Cs_xH_{3-x}PW_{12}O_{40}$ was studied recording the TG, DTG, DTA and T curves during experiments. The adsorption of ethanol at 100 ^oC on H_3PW, Cs_1H_2PW, Cs_2H_1PW and $Cs_{2.25}H_{0.75}PW$ take place exclusively on Brönsted acid sites by hydrogen bonds formation, unlike the Cs_3PW where physisorption prevails. In the $Cs_{2.5}H_{0.5}PW$ case there is a significant quantity of physisorbed ethanol together with hydrogen bonded ethanol. The subsequent desorption take place from Brönsted acid sites in similar way with crystallization water removal. The highest desorbed ethanol on $Cs_{2.25}H_{0.75}PW$ and $Cs_{2.5}H_{0.5}PW$ of 1, respectively 1.4 $EtOH/H^+$ could be a result of easier access to the Brönsted acid sites. The results of the adsorption at 300 ^oC show that ethanol reacts during adsorption/desorption steps with formation of strongly adsorbed species, reduction of the solids and carbonaceous deposit formation. The deactivation as result of the strongly adsorbed species and the carbonaceous deposit is discussed.

(Received February 24, 2012; accepted June 6, 2012)

Keywords: Tungstophosphoric acid, Tungstophosphates of Cs, Adsorption-desorption of ethanol

1. Introduction

In the last time much attention has been paid to biomass as alternative resource to petroleum, since biomass is a renewable resource and its combustion does not lead to increased CO_2 in the atmosphere. Ethanol is one of the main biomass-derived products [1, 2]. The search for renewable resources has stimulated hydrocarbons production from ethanol over different acidic solid catalysts [3-12]. The $H_3 PW_{12}O_{40}$ and its salts, especially with Cs, are effective catalysts in ethanol conversion to ethylene [3-7, 12] and the reaction kinetics is interesting to the catalysis theory and industrial application also. The dehydration of ethanol on strong acidic catalysts involves the ethanol adsorption and in consequence a complex series of reactions (oligomerization, aromatization, cracking and hydrogenation) occurred. In purpose to understand the dehydration and secondary reactions mechanism on $Cs_xH_{3-x}PW_{12}O_{40}$ as catalysts, the adsorption of ethanol and its temperature programmed desorption–TPD using thermogravimetry were studied.

2. Experimental

The tungstophosphoric acid $H_3[PW_{12}O_{40}]\cdot xH_2O$ (H_3PW) was synthesized according to the methods described of J. C. Bailar (Inorg. Synth., 1, 1939, 132-133) and M. Misono et. al. (Bull. Chem. Soc. Jpn., 55, 1982, 400-406) and it was described in detail elsewhere [13]. The salts of H_3PW with Cs content of 1, 2, 2.25, 2.5 and 3 ($Cs_xH_{3-x}PW_{12}O_{40}$) were prepared by precipitation from an aqueous solution of the parent acid adding the required stoichiometric quantity of counter-ion salts as caesium nitrate under stirring as was reported previously [13]. The humidity and crystallization water content of all prepared heteropoly compounds was determined by thermal analysis after their keeping in air at room temperature until constant weight was observed.

The thermal analyses were carried out with the Mettler TGA/SDTA 851/LF/1100 thermo analyser. The measurements were conducted in dynamic atmosphere of synthetic air (50 ml/min), using the alumina plates crucibles of 150 µl. Heating rate was 10 °C/min and the mass samples were about 30 mg.

Specific surface and porosity measurement by BET method were calculated from the nitrogen adsorption-desorption isotherms, using Nova 1200 Quantachrome equipment**.** The sample was previously degassed to 10^{-5} Pa at 250 ^oC for 2 h.

The adsorption of ethanol at 100 ^oC and temperature programmed desorption procedure were carried out with the same Mettler TGA/SDTA 851/LF/1100 thermo analyser used for the thermal analysis and it consists of the next steps**:**

(1) non-isothermal heating from 25 to 300 ^oC with 10 ^oC/min, under air flow of 50 mL/min;
(2) isothermal heating at 300 ^oC, 30 min, under air flow of 50 mL/min;
(3) cooling from 300 to 100 ^oC with 10 ^oC/min, under nitrogen flow of 50 mL/min;
(4) isothermal heating at 100 ^oC for ethanol adsorption, under a flow of 50 mL/min consist of nitrogen +8 % ethanol, 120-180 min, function of the required time to reach constant mass;
(5) isothermal heating at 100 ^oC, under a nitrogen flow of 50 mL/min, 120–300 min, to remove excess of ethanol;

(6) non-isothermal heating from 100 to 550 °C, with 10 °C/min, under nitrogen flow of 50 mL/min;
(7) isothermal heating at 550 °C, 60 min, under 50 mL/min of nitrogen flow;
(8) isothermal heating at 550 °C, 60 min, under 50 mL/min of air flow for to check up the formation of organic deposits on heteropoly compounds.
The same procedure was applied for the adsorption at 300 °C and for the subsequent temperature programmed desorption.

3. Results

The thermal decomposition of the $H_3PW{\cdot}xH_2O$ and its acid Cs salts takes place between 25 °C and about 600 °C. The thermal analysis of the $H_3PW{\cdot}xH_2O$ shows the loss of water in three steps (Fig. 1-3). The first one corresponds to the loss of the physical adsorbed water and the water molecule bound by hydrogen weak bonds in the temperature range of 25-110 °C. The second step corresponds to the water molecules of $H_5O_2^+$ expelled in the range of 110-300 °C as in the $H_3PW{\cdot}6H_2O$ all the 6 water molecules are bonded of H^+. The third step is the constitutional water loss, over 300 °C (the water formed of the protons and the oxygen of the $[PW_{12}O_{40}]^{3-}$-named Keggin Unit-KU). The TG-DTA experiments have shown the complete elimination of the physical adsorbed water and the crystallization water from $H_3PW{\cdot}xH_2O$ and its acidic salts after isothermal heating at 300 °C for 1 h. The mass loss corresponding to the segment 1-2 from TG curve gives very close values to the theoretical ones for the constitutional water content for all compounds (the number of protons are equal to the double of the constitutional water molecules). In the Cs_3PW case only the physical adsorbed water was observed, as it can be seen in the Fig. 3.

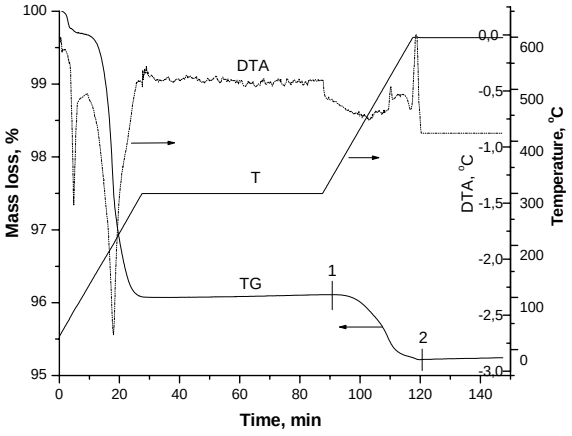

Fig. 1. The TG, DTA curves and the temperature heating program-T curve for H_3PW.

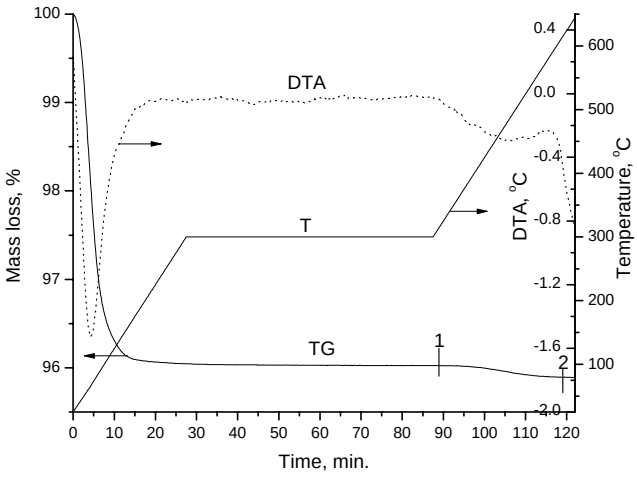

Fig. 2. The TG, DTA curves and the temperature heating program-T curve for $Cs_{2.5}H_{0.5}PW$.

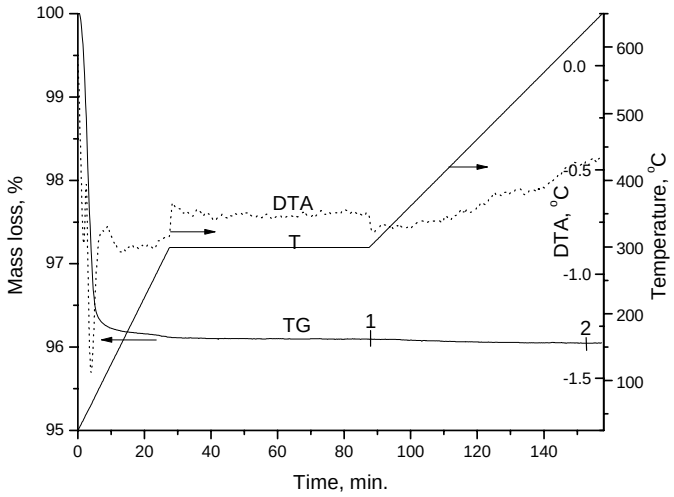

Fig. 3. The TG, DTA curves and the temperature heating program-T curve for Cs_3PW.

The specific surface area and pore volume of the studied compound were determined on the basis of the BET measurements, which showed an abrupt increase in the specific surface area with the decrease of H^+ content below 1 H^+/KU. It was calculated 1-7 m^2/g, for $H^+>2$ and 50-140 m^2/g for $H^+\leq 2$ (Fig. 4). The pore volume of the samples increased nearly in the same way. These results are supported by earlier findings [14, 15]. The size of the aggregates was calculated from electron diffractogram patterns.

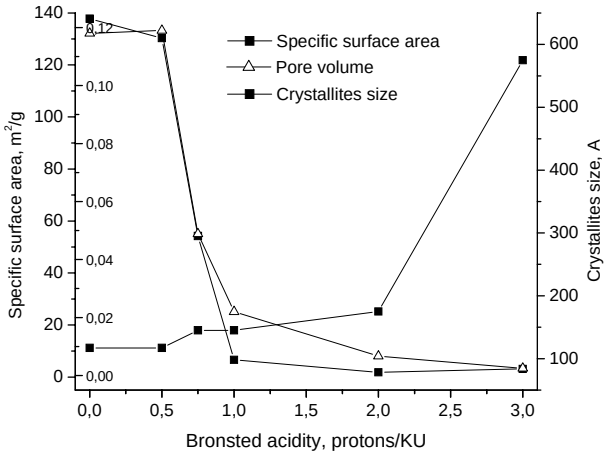

Fig. 4. The specific surface area, pores volume and crystallites size of the $Cs_xH_{3-x}PW_{12}O_{40}$ ($Cs_xH_{3-x}PW$), x=1, 2, 2.25, 2.5 and 3 depending on the Protons/ $PW_{12}O_{40}^{3-}$ (KU) ratios.

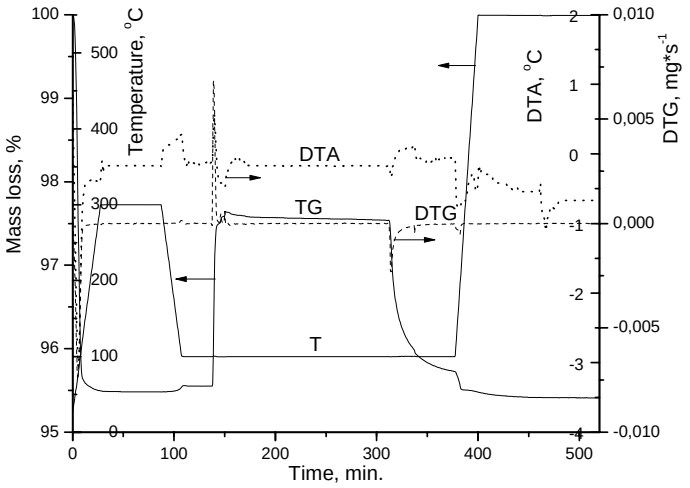

Fig. 6. The thermal curves recorded during crystallization water removal and adsorption (at 100 °C) /desorption of ethanol on $Cs_{2.5}H_{0.5}PW$.

The TPD experiments were recorded as the TG, DTG, DTA and T curves. Typical results are shown in Fig. 5-7 for adsorption at l00 °C, respectively Fig. 8-10 for adsorption at 300 °C. In the first part of the TG curves (Fig. 5-7) arises a plateau for the isothermal heating at 300 °C, corresponding to the complete removal of crystallization water and the formation of anhydrous forms of the studied compounds. The other two plateaus on TG curves correspond to saturation with ethanol at l00 °C, respectively to the stable chemisorbed species of ethanol at 100 °C can be observed. The heating of the sample carrying on from l00 °C to 550 °C pointed out an ethanol desorption process and the constitutional water release. In the last stage of experiments, during the isothermal heating at 550 °C, under flowing air (50 mL/min), no significant increase or decrease of mass were pointed out on TG curves of fig. 5-7. The results of adsorption/desorption experiments in the temperature range of 100–550 °C are summarized in Table 1. A good correspondence between the number of proton/KU and the constitutional water loss is pointed out.

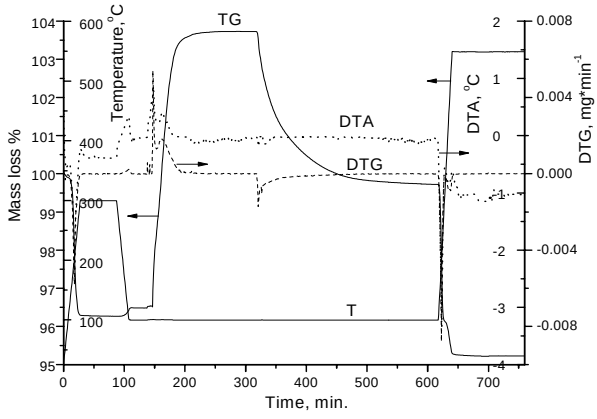

Fig. 5. The thermal curves recorded during crystallization water removal and adsorption (at 100 °C) /desorption of ethanol on H_3PW.

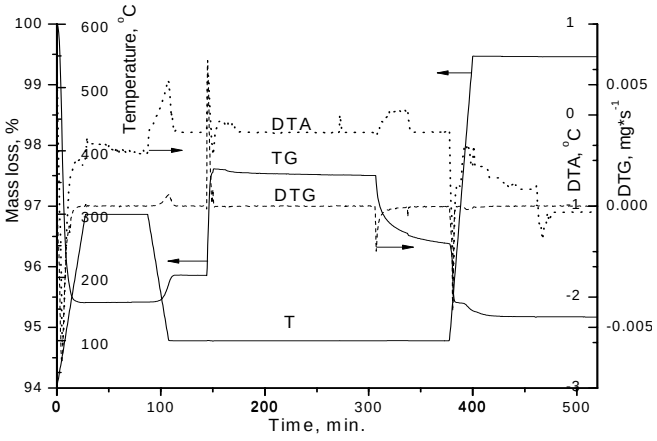

Fig. 7. The thermal curves recorded during crystallization water removal and adsorption (at 100 °C) /desorption of ethanol on $Cs_{2.5}H_{0.5}PW$.

This means there is no organic deposit on HPCs at the end of desorption, then all organic species formed at desorption were removed, otherwise, a significant mass loss and an exothermic effect by coke burning have to be noticed. Also no reduction occurred during adsorption/desorption processes as no mass increase by reoxidation under flow of air was observed. Unlike the results of adsorption at l00 °C, after adsorption at 300 °C, the 1st and 2nd steps of desorption do not appear, a new step of desorption and new processes of mass increase, respectively mass decrease, during air let in arise (Fig 8-10). The last processes were assigned to reoxidation of the solid compounds, respectively the burning of carbonaceous deposit formed on the solid compounds during adsorption/desorption of ethanol. All these processes are summarized in the Table 2.

Table 1. The processes of adsorption (at 100 °C) /desorption of ethanol on the $Cs_xH_{3-x}PW_{12}O_{40}$.

	Adsorption, EtOH/KU	1st Desorption step		2nd Desorption step		Constitutional water release	
		EtOH/ KU	Temp., °C	EtOH/ KU	Temp., °C	H_2O/ KU	Temp., °C
H_3PW	4.9	2.6	100	2.3	100-323	1.58	323-550
Cs_1H_2PW	2.7	1.11	100	1.55	100-316	1.06	316-550
Cs_2H_1PW	1.4	0.56	100	0.78	100-315	0.51	315-550
$Cs_{2.25}H_{0.75}PW$	1.29	0.56	100	0.73	100-318	0.40	318-550
$Cs_{2.5}H_{0.5}PW$	1.59	0.82	100	0.71	100-325	0.25	325-550
Cs_3PW	1.53	1.35	100	0.16	100-326	0.00	-

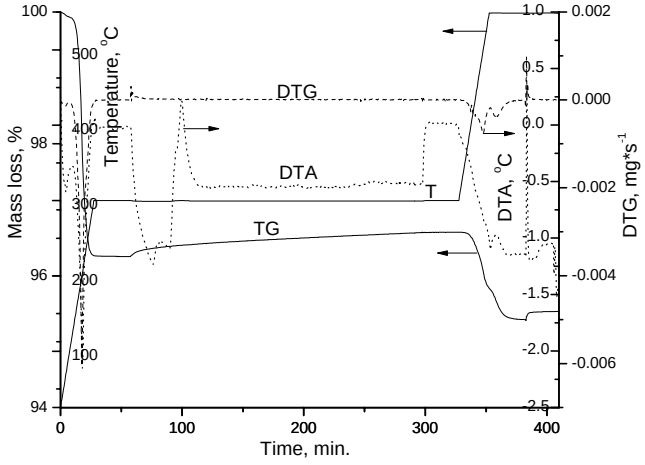

Fig. 8. The thermal curves recorded during crystallization water removal and adsorption (at 100 °C) /desorption of ethanol on H_3PW.

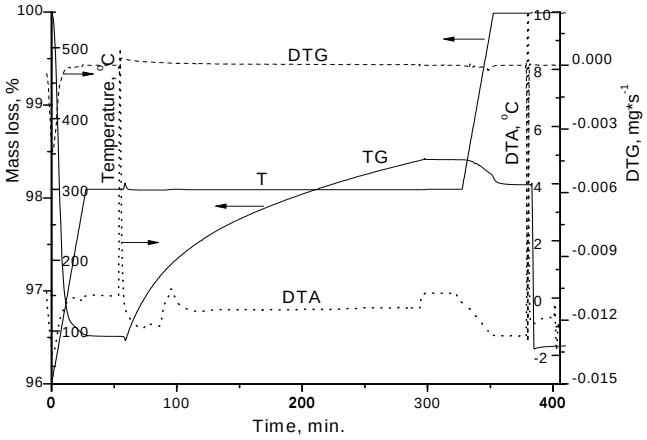

Fig. 9. The thermal curves recorded during crystallization water removal and adsorption (at 300 °C) /desorption of ethanol on $Cs_{2.5}H_{0.5}PW$.

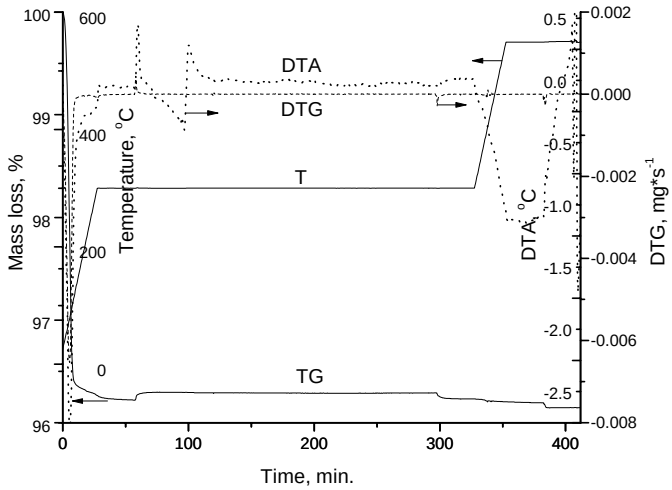

Fig 10. The thermal curves recorded during crystallization water removal and adsorption (at 300 °C) /desorption of ethanol on Cs_3PW.

Table 2. The processes of adsorption (at 300 °C) /desorption of ethanol on the $Cs_xH_{3-x}PW_{12}O_{40}$.

	Adsorption, EtOH/KU	1st Des. step	2nd Des. step	Constitutional water release		3rd Des. step		(+)Reoxidation/ (-)Carbon burning	
		EtOH/ KU	EtOH/ KU	H_2O/ KU	Temp., °C	EtOH /KU	Temp., °C	(+)4O/KU (-)EtOH/KU	Temp., °C
H_3PW	0.24	-	-	1.45	321-550	0.30	550	(+)0.06	550
Cs_1H_2PW	0.16	-	-	0.95	321-550	0.18	550	(+)0.02	550
Cs_2H_1PW	0.42	-	-	0.51	316-550	0.18	550	(-)0.26	550
$Cs_{2.25}H_{0.75}PW$	1.02	-	-	0.40	317-550	0.080	550	(-)1.03	550
$Cs_{2.5}H_{0.5}PW$	1.37	-	-	0.27	320-550	0.085	550	(-)1.26	550
Cs_3PW	0.051	0.046	-	0.05	320-550	0.010	550	(-)0.030	550

Legend: (+) mass increase, (-) mass decrease

4. Discussion

The catalytic properties of solid compounds are in tight relation with composition, structure, texture and adsorption capacity of reactants. The last properties at it turn depends strongly of composition, structure and texture.

The $Cs_xH_{3-x}PW_{12}O_{40}$ consist of Keggin Units, as primary structure, so the composition could be check easy as the KU gives IR bands like a "truthful fingerprint". Thus, only the characteristic bands of the Keggin Unit ($\nu_{as}P\text{-}O_i\text{-}W$, 1080-1081; $\nu_{as}W\text{-}O_t$, 976-995; $\nu_{as}W\text{-}O_c\text{-}W$, 890-900; $\nu_{as}W\text{-}O_e\text{-}W$, 805-810 cm^{-1} [16], respectively , $\nu_{as}P\text{-}O_i\text{-}W$, 1079; $-\nu_{as}W\text{-}O_t$, 975; $\nu_{as}W\text{-}O_c\text{-}W$, 887; $\nu_{as}W\text{-}O_e\text{-}W$, 795 cm^{-1} in H_3PW and $\nu_{as}P\text{-}O_i\text{-}W$, 1080; $-\nu_{as}W\text{-}O_t$, 985; $\nu_{as}W\text{-}O_c\text{-}W$, 890; $\nu_{as}W\text{-}O_e\text{-}W$, 804 cm^{-1} in $C_{2.7}H_{0.3}PW$ [17]) were observed in all studied compounds. Also, the all characteristic bands of the KU are still observed for heated samples at 573 °C. The increase of Cs content causes an increase of thermal stability, thus, the primary structure was preserved until 600 °C for the Cs_1H_2PW, Cs_2H_1PW and $Cs_{2.5}H_{0.5}PW$ as all characteristic IR bands are still present at this temperature unlike to H_3PW, as it was reported previously in detail elsewhere [13]. The proton number could be easy calculated from the constitutional water loss as it was mentioned before.

The secondary structure of the $H_3PW{\cdot}6H_2O$ and their Cs salts belong to cubic system-Pn3m symmetry [18]. The X-ray diffraction spectra of the studied compounds exhibit the reflections corresponding to cubic crystalline structure only. The X-ray diffraction spectra of samples heated at 600 °C for the H_3PW have evidenced the complete decomposition to corresponding oxides and the WO_3 crystallization. On the other hand, the WO_3 is present in all acidic salts diffraction spectra heated at 600 °C, as its main characteristic line (100) was observed in their spectra. The intensity of this band decreases with respect to Cs content increasing [13].

The acidic salts microstructure as mixture of H_3PW and Cs_3PW in various ratios function of Cs content was sustained based on the following observations on the samples heated at 600 °C: - the presence of specific IR bands for KUs in the IR spectra of the all salts and their disappearance of the $H_3PW{\cdot}6H_2O$ spectrum; - the presence of the reflections corresponding to cubic secondary structure of KUs arrangements together with the characteristic reflections of WO_3 from the XRD spectra of the acidic salts; - only the presence of characteristic reflections to WO_3 in XRD spectrum of $H_3PW{\cdot}6H_2O$ [13].

The texture data of the studied compounds (Fig. 3) support the microstructure model of mixture between H_3PW and Cs_3PW for the acidic salts as a core of Cs_3PW aggregates embedded of H_3PW layers [15]. The slight change of the aggregates size for the $H^+/KU \geq 2$ shows that it is not the reason for the abrupt increases in the specific surface area and the pore volume, so the lower numbers of H_3PW layers could be the ground for sharp increase of the pore volume and specific surface area as the pores between aggregates of Cs_3PW are filled more or less with H_3PW.

The heteropoly compounds-HPCs as H_3PW and its salts have a behaviour of so-called "pseudo-liquid phase" as it absorb easily in volume polar molecules like water, alcohols, amines and do not absorb non-polar molecules as hydrocarbons [14, 19].

On the basis of these assumptions the results of the adsorption at 100°C and the subsequent desorption could be explained thus:

- The adsorption of ethanol on H_3PW, Cs_1H_2PW, Cs_2H_1PW and $Cs_{2.25}H_{0.75}PW$ take place exclusively on Brönsted acid sites by hydrogen bonds formation, similar with binding of crystallization water, unlike the Cs_3PW where physisorption prevails. In the $Cs_{2.5}H_{0.5}PW$ there is a significant quantity of physisorbed ethanol, as the adsorbed ethanol decreases from H_3PW to $Cs_{2.25}H_{0.75}PW$ and increase for $Cs_{2.5}H_{0.5}PW$ (see Table 1).

- The desorbed ethanol in 2nd step is about 0.8 $EtOH/H^+$ on H_3PW, Cs_1H_2PW, Cs_2H_1PW and about 1 on $Cs_{2.25}H_{0.75}PW$, respectively 1.4 on $Cs_{2.5}H_{0.5}PW$, which could be a result of easier access to the Brönsted acid sites in the last two cases.

The ethanol balance for adsorption and desorption processes is very good, the differences are below 5%. As was mentioned before no burning of organic deposit on HPCs and no reoxidation under flow of air were observed.

The results of the adsorption at 300 ^{o}C (summarized in Table 2) point out during adsorption/desorption steps, the ethanol reactions accompanied of the HPCs reduction and carbonaceous deposit formation. These processes were pointed out through reoxidation of the solid compounds, respectively through the burning of carbonaceous deposit. The reoxidation process was observed only on H_3PW and Cs_1H_2PW, but it have to occur in all cases. It can't be observed in the other cases as result of a less reduced KU ratio and the burning of carbonaceous deposit process which overlays the reoxidation. The strongly adsorbed species corresponding to the 3rd step of desorption decreases from H_3PW to Cs_3PW, while the carbonaceous deposit increase from Cs_2H_1PW to $Cs_{2.5}H_{0.5}PW$ and decrease on Cs_3PW. Both, the strongly adsorbed species corresponding to the 3rd step of desorption and carbonaceous deposit are results of ethanol reactions and it still remains on solid after constitutional water removal. In the main, the adsorbed EtOH/KU corresponds with the sum of: - the desorbed EtOH/KU (3rd step); - the reoxidation (expressed as 4O/KU) with minus and the burning of carbonaceous deposit (expressed as EtOH/KU). The oxygen for reoxidation per KU was calculated on the basis of the oxygen used in the reaction (2):

$$C_2H_5OH = C_2H_4 + H_2O \quad (1)$$

$$C_2H_4 + 2O_2 = 2CO + 2H_2O \quad (2)$$

It have to be noticed, the mass loss between 320 and 550 ^{o}C on Cs_3PW corresponding to constitutional water release. It could be explain by some few W^{6+} ions reduction and the equivalent number of H^+ arises from water decomposition for electric charge compensation during adsorption at 300 ^{o}C.

On the basis of these results could be explained the high catalytic activity of alcohol conversion on all compounds, especially on the $Cs_{2.5}H_{0.5}PW$ [7] and a supposed deactivation process on H_3PW as the strongly adsorbed species will block the access in the deeper layers of crystal aggregates and less Brönsted acid sites which will act, consequence of its low specific surface area. The effect of the carbonaceous deposit on the catalytic activity of the $Cs_{2.25}H_{0.75}PW$ and $Cs_{2.5}H_{0.5}PW$ could be less important as result of its high specific surface area.

5. Conclusions

The adsorption of ethanol at 100 ^{o}C on H_3PW, Cs_1H_2PW, Cs_2H_1PW and $Cs_{2.25}H_{0.75}PW$ take place exclusively on Brönsted acid sites by hydrogen bonds formation, similar with binding of crystallization water, unlike the Cs_3PW where physisorption prevails. In the $Cs_{2.5}H_{0.5}PW$ case there is a significant quantity of physisorbed ethanol together with hydrogen bonded ethanol.

The subsequent desorption take place from Brönsted acid sites, similar with crystallization water removal. The desorbed ethanol of about 0.8 EtOH/H^+ on H_3PW, Cs_1H_2PW and Cs_2H_1PW and about 1 on $Cs_{2.25}H_{0.75}PW$, respectively 1.4 on $Cs_{2.5}H_{0.5}PW$ could be a result of easier access to the Brönsted acid sites in the last two cases.

The results of the adsorption at 300 ^{o}C show that ethanol reacts during adsorption/desorption steps with formation of strongly adsorbed species, reduction of the solids and carbonaceous deposit formation. Both, the strongly adsorbed species and carbonaceous deposit still remain on solid after constitutional water removal.

The reoxidation of solid was observed only on H_3PW and Cs_1H_2PW, but it have to occur in all cases. It can't be observed in the other cases as result of a less reduced KUs ratio and the burning of carbonaceous deposit which overlays the reoxidation process.

On the basis of these results could be explained the high catalytic activity of ethanol conversion on all compounds, especially on $Cs_{2.5}H_{0.5}PW$ and it could be expected a significant deactivation process on H_3PW as the strongly adsorbed species will block the access in the deeper layers of crystal aggregates and less Brönsted acid sites which will act, consequence of its low specific surface area. The effect of the carbonaceous deposit on the catalytic activity of the $Cs_{2.25}H_{0.75}PW$ and $Cs_{2.5}H_{0.5}PW$ could be less important as result of its high specific surface area.

Acknowledgment

The authors would like to thank to the Romanian Academy for financial support by Academic

Research Programme and to the CBC Hungary-Romania programme (HURO /0901/090/2.2.2 project) that allow us to finish this work

References

[1] Yan Lin, Shuzo Tanaka, Appl Microbiol. Biotechnol., **69**, 627 (2006).
[2] F. Ben Chaabane, A. S. Aldiguier, S. Alfenore, X. Cameleyre , P. Blanc, C. Bideaux, S. E. Guillouet, G. Rou, C. Molina-Jouve, Bioprocess Biosyst Eng **29**, 49 (2006).
[3] J. B. McMonagle, J. B. Moffat, J. Catal. **91**, 132 (1985).
[4] J. G. Highfield, J. B. Moffat, J. Catal., **98**, 245 (1986).
[5] M. Misono, T. Okuhara, T. Ichiki, T. Arai, Y. Kanda, J. Am. Chem. Soc., **109**, 5535 (1987).
[6] K. Y. Lee, T. Arai, S. Nakata, S. Asaoka, T. Okuhara, M. Misono, J. Am. Chem. Soc., **114**, 2836 (1992).
[7] N. Mizuno, M. Misono, Chem. Rev., **98**, 199 (1998).
[8] A. Yee, S. J. Morrison, H. Idriss, J. Catal. **186**, 279 (1999).
[9] M. Inaba, K. Murata, M. Saito, I. Takahara, React. Kinet, Catal. Lett., **88**, 135 (2006).
[10] N. R. C. F. Machado, V. Calsavara, N. G. C. Astrath, A. M. Neto, M. L. Baesso, Appl. Catal. A: General **311**, 193 (2006).

[11] R. V. Ermakov, V. A. Plakhotnik, Petroleum Chemistry, **48**, 1 (2008).
[12] L. Matachowski, A. Zieba, M. Zembala, A. Drelinkiewicz, Catal. Lett., **133**, 49 (2009).
[13] V. Sasca, O. Verdes, L. Avram, A. Popa, P. Barvinschi, M. Mracec, Rev. Roum. Chim. **56**, 501 (2011).
[14] M. Misono, N. Mizuno, K. Katamura, A. Kasai, Y. Konishi, K. Sakata, T. Okuhara, Y. Yoneda, Bull. Chem. Soc. Jpn., **55**, 400 (1982).
[15] T. Okuhara, T. Nakato, Catalysis Surveys from Japan, **2**, 31 (1998).
[16] C. Rocchiccioli-Deltcheff, M. Fournier, R. Franck R. Thouvenot, Inorg. Chem. **22**, 207 (1983).
[17] N. Essayem, A. Holmqvist, P.Y.Gayraud, J.C. Vedrine and Y.B. Taarit, J. Catal., **197**, 273 (2001).
[18] G. M. Brown, M.-R. Noe-Spirlet, W.A. Busing H.A. Levy, Acta cryst. *B,* **33**, 1038 (1977).
[19] T. Okuhara, S. Tatematsu, K. Y. Lee, M. Misono, Bull. Chem. Soc. Jpn., **62**, 717 (1989).

*Corresponding author: orsinaverdes@yahoo.com